Biomaterials Science

ROYAL SOCIETY OF CHEMISTRY

REVIEW

View Article Online
View Journal | View Issue

Cite this: *Biomater. Sci.*, 2025, **13**, 858

Integrating 3D printing of biomaterials with nitric oxide release†

Herllan V. de Almeida,[a] Mateus P. Bomediano,[a] Daniele M. Catori,[b] Elizaura H. C. Silva[a] and Marcelo G. de Oliveira *[a]

The pivotal roles played by nitric oxide (NO) in tissue repair, inflammation, and immune response have spurred the development of a wide range of NO-releasing biomaterials. More recently, 3D printing techniques have significantly broadened the potential applications of polymeric biomaterials in biomedicine. In this context, the development of NO-releasing biomaterials that can be fabricated through 3D printing techniques has emerged as a promising strategy for harnessing the benefits of localized NO release from implantable devices, tissue regeneration scaffolds, or bandages for topical applications. Although 3D printing techniques allow for the creation of polymeric constructs with versatile designs and high geometric precision, integrating NO-releasing functional groups or molecules into these constructs poses several challenges. NO donors, such as *S*-nitrosothiols (RSNOs) or diazeniumdiolates (NONOates), may release NO thermally, complicating their incorporation into resins that require heating for extrusion-based 3D printing. Conversely, NO released photochemically from RSNOs effectively inhibits radical propagation, thus hindering photoinduced 3D printing processes. This review outlines the primary strategies employed to overcome these challenges in developing NO-releasing biomaterials *via* 3D printing, and explores future prospects in this rapidly evolving field.

Received 29th September 2024,
Accepted 6th January 2025

DOI: 10.1039/d4bm01304b

rsc.li/biomaterials-science

[a]*Institute of Chemistry, University of Campinas, UNICAMP, Campinas 13083-970, São Paulo, Brazil. E-mail: mgo@unicamp.br*
[b]*School of Chemical, Materials and Biomedical Engineering, College of Engineering, University of Georgia, Athens 30602, Georgia, USA*
† Electronic supplementary information (ESI) available. See DOI: https://doi.org/10.1039/d4bm01304b

Introduction

Nitric oxide (NO), synthesized endogenously in mammals, plays crucial roles in numerous biological processes, such as vasodilation and blood pressure regulation, angiogenesis, inhi-

Herllan V. de Almeida

Herllan Vieira de Almeida received his Master's degree in Chemistry in 2022 from the University of Campinas (UNICAMP), Brazil. He is currently a PhD candidate in Science at the Institute of Chemistry (UNICAMP), focusing on the development of nitric oxide (NO)-releasing organic–inorganic hybrid resins for use in photoinduced 3D printing for the fabrication of blood-contacting medical devices with anti-thrombotic surfaces. He is a member of the Nitric Oxide & Biomaterials group led by Prof. Marcelo G. de Oliveira, whose focus is on the development of NO-releasing polymeric biomaterials.

Mateus P. Bomediano

Mateus Peres Bomediano earned his undergraduate degree in Chemistry from the University of Campinas (UNICAMP), Brazil, in 2021. He is currently a PhD candidate and a member of the Nitric Oxide & Biomaterials Group, led by Prof. Marcelo G. de Oliveira at UNICAMP's Institute of Chemistry. His research focuses on developing 3D-printable nitric oxide (NO)-releasing vascular prostheses using photocrosslinkable micellar hydrogels. Mateus is currently conducting an internship at the Physical-Chemistry Department at Lund University, Sweden, where he is specializing in characterizing micellar systems using Small Angle X-ray Scattering (SAXS).

bition of thrombus formation, immune response, wound healing, and bone tissue regeneration. The diverse biological actions of NO have driven the development of various biomaterials designed to release NO locally, thereby harnessing its potential therapeutic benefits for medical applications.[1–3]

Given that NO is a gaseous and reactive radical species, its release from biomaterials typically involves either loading the materials with NO-releasing molecules or directly functionalizing polymeric chains of the biomaterial matrix with NO-releasing functional groups. In both approaches, the primary objective has been to develop stable NO-donor biomaterials, where NO release can be effectively triggered by external stimuli such as temperature changes, visible or ultraviolet light irradiation, metal catalysts, or pH variations.[4] There are several classes of NO donors, each offering a distinct range of NO-releasing properties and chemical behaviors, making them suitable for various biomedical applications. Sodium nitroprusside, a well-known metal-nitrosyl complex (Metal-NO), is one of the most consolidated NO donor drugs in medicine, widely used as a vasodilator during surgeries and for managing hypertensive crises. Beyond metal-nitrosyl complexes, the two other primary classes of NO-releasing molecules are the diazeniumdiolates (NONOates) and the *S*-nitrosothiols (RSNOs).[5] These compounds have been largely utilized as experimental NO donors in biomaterials, either through physical incorporation into polymer matrices or chemically binding them to polymer chains.

Additive manufacturing, through 3D printing techniques, has emerged as a promising technology in various biomedical applications, including tissue engineering,[6] regenerative medicine,[7] and the development of implantable devices.[8] Its application in such biomedical contexts has addressed the growing demand for personalized medicine, enabling, for example, the production of implants tailored to individual patients. Additive manufacturing offers high precision, efficiency, and fidelity in creating complex, custom-designed constructs based on 3D computer models.[9] By merging the customization capabilities of 3D printing with the incorporation of NO donors into the obtained constructs, new avenues can be explored in developing biomaterials with diverse biological functionalities.

In this review, we summarize the biological and therapeutic properties of NO, focusing particularly on the use of RSNOs and NONOates as NO donor molecules and their incorporation into polymeric matrices of biomaterials. We also describe the key concepts, material requirements, and mechanisms underlying the main 3D printing techniques, in the context of developing NO-releasing biomaterials. Finally, we describe the state of the art in obtaining NO-releasing biomaterials through 3D printing techniques, as well as the challenges to be overcome in integrating these two concepts.

Nitric oxide actions

The discovery in the 1980s of the endogenous production of NO in mammalian cells and its role as a signaling molecule in the vascular system significantly heightened interest in NO research, particularly in the development of materials and devices for biological applications.[10] NO, a gaseous free radical, plays a critical role in numerous physiological and pathophysiological processes. Its endogenous production is mediated by enzymes known as nitric oxide synthases (NOS), which catalyse the conversion of L-arginine to L-citrulline, releasing NO as a byproduct of this reaction.[11] At low concentrations (<1–30 nM), NO supports a range of beneficial physiological effects, including vasodilation, angiogenesis, cell proliferation, and anti-inflammatory, antiplatelet, and anticoagulant activities. However, when present in higher concentrations (>1 μM), particularly under conditions of oxidative stress, NO can react with dioxygen and superoxide ($O_2^{\bullet-}$),

Daniele M. Catori

Daniele Mayara Catori earned her Master's degree in Chemistry from the State University of Maringá, Brazil, in 2019, and her PhD in Science from the University of Campinas (UNICAMP), Brazil, in 2023. As a former member of the Nitric Oxide & Biomaterials Group led by Prof. Marcelo G. de Oliveira at UNICAMP's Institute of Chemistry, she developed photocrosslinkable and 3D-printable injectable hydrogels for localized nitric oxide (NO)-delivery in cartilage replacement and regeneration. She is currently a postdoctoral researcher at the School of Chemical, Materials, and Biomedical Engineering, College of Engineering, University of Georgia, Athens, USA.

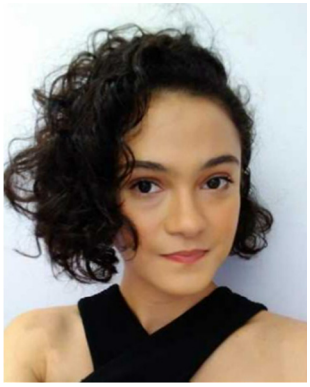

Elizaura H. C. Silva

Elizaura Hyeda Carvalho Silva earned her Master's degree in Analytical Chemistry in 2020 from the Federal University of Maranhão, Brazil. She is currently a PhD candidate in Science at the Institute of Chemistry, University of Campinas (UNICAMP), Brazil. Her research focuses on developing photocrosslinkable bioabsorbable resins for the photo-induced 3D printing of self-expandable nitric oxide (NO)-releasing intracoronary stents. She is a member of the Nitric Oxide & Biomaterials Group, led by Prof. Marcelo G. de Oliveira, which specializes in creating NO-releasing polymeric biomaterials for advanced medical applications.

leading to the formation of reactive nitrogen species (RNS) such as nitrogen dioxide (NO_2), dinitrogen trioxide (N_2O_3), and peroxynitrite ($ONOO^-$).[12] These reactive species can induce cytotoxic effects, contributing to nitrosative stress, inflammation, and tissue damage. In certain pathological conditions, such as infections, the overproduction of NO by inducible nitric oxide synthase (iNOS) can exacerbate tissue damage and organ dysfunction. Recent studies have demonstrated that elevated concentrations of NO (500 nM to 2 μM) in the tumor microenvironment (TME) are linked to nitrosative stress signaling. This signaling cascade induces cancer cell cycle arrest, apoptosis, and inhibition of glycolysis. These findings support the hypothesis that therapeutic administration of NO at sufficiently high concentrations may not only exert anti-cancer effects but also enhance the efficacy of chemotherapy and radiotherapy.[13] In addition, localized NO delivery at high concentrations has been demonstrated to possess antimicrobial properties. The microbicidal effects of NO may involve the disruption of bacterial DNA or the degradation of cyclic diguanylate (cyclic di-GMP), a key signaling molecule responsible for maintaining biofilm integrity in many bacterial species.[14,15]

Polymeric materials capable of releasing NO at rates between 0.5 and 20×10^{-10} mol min^{-1} cm^{-2} have been shown to effectively eliminate both Gram-positive and Gram-negative bacteria without inducing cytotoxic effects on the surrounding tissue cells.[16] Conversely, materials that release NO at slower rates have been found to promote angiogenesis, as well as enhance cell proliferation and migration, thereby accelerating wound healing and tissue regeneration.[17,18] Thus, precise control over the rate of NO delivery from biomaterials is critical for achieving specific therapeutic outcomes, whether for antimicrobial purposes or for tissue repair and regeneration.

In immunopharmacology, NO plays a crucial role in modulating inflammatory processes by inhibiting the activation of NF-κB, a key transcription factor responsible for the expression of genes involved in inflammation, including those encoding cytokines, chemokines, and adhesion molecules.[19] Additionally, NO exhibits potent antioxidant properties by neutralizing superoxide and other reactive oxygen species (ROS),[20] thereby reducing oxidative stress. Materials engineered to release NO have demonstrated the ability to modulate the release of inflammatory mediators, leading to a reduction in nitrosative stress and offering antinociceptive effects. This makes NO-releasing materials promising candidates for therapies aimed at controlling inflammation and alleviating pain.[21,22]

Marcelo G. de Oliveira

Marcelo Ganzarolli de Oliveira earned his PhD in Science from the University of Campinas (UNICAMP), Brazil in 1992. He is a Full Professor at UNICAMP's Institute of Chemistry and leads the Nitric Oxide & Biomaterials group. His research focuses on the development of nitric oxide (NO)-releasing polymeric biomaterials and their physiological effects. His team has developed functionalized polymers and hydrogels for localized NO release and coating implantable medical devices. Recently, his group has applied 3D printing to create topical and implantable NO-releasing medical devices, advancing the design and functionality of biomaterials for therapeutic applications.

S-Nitrosothiols as a NO donors

The exogenous administration of NO presents challenges due to its low water solubility and instability in the presence of oxidizing agents. To address these issues, various controlled release strategies have been developed, including the physical incorporation of NO donors into materials,[23] the introduction of enzymes or molecules that stimulate *in situ* NO production,[24] and the functionalization of polymer chains to modulate NO release.[4,25]

Among the most used NO donors in biomaterials are the RSNOs, which spontaneously release NO in response to light and/or heat. These donor molecules can be synthesized in aqueous media through the *S*-nitrosation of thiol (–SH) groups of endogenously found molecules such as glutathione (GSH) and albumin, or synthetic precursors like *N*-acetyl-DL-penicillamine (NAP). The *S*-nitrosating process typically involves nitrosating agents, such as nitrous acid (HNO_2), which is formed by the protonation of nitrite (NO_2^-) in acidified aqueous solutions.[11,26,27] These approaches are pivotal in the design of NO-releasing biomaterials for various therapeutic applications, as they enable precise control over NO delivery, enhancing the efficacy and safety of NO-based treatments.

The natural presence of RSNOs in the human body suggests they may pose fewer toxicity concerns compared to other exogenous NO donors, such as NONOates and Metal-NO complexes. However, RSNOs tend to have limited stability both *in vitro* and *in vivo*, which has driven researchers to incorporate them into polymeric matrices to enhance their stability and control the release of NO.[11,28] Depending on their solubility, NO donors can be integrated into these matrices through physical absorption from solution. For instance, the hydrophobic *S*-nitroso-*N*-acetyl-DL-penicillamine (SNAP) can be embedded into materials by immersing the dry substrate in an alcoholic solution of SNAP.[29,30] Similarly, hydrophilic RSNOs, such as *S*-nitrosoglutathione (GSNO) and *S*-nitroso-*N*-acetylcysteine (SNAC), can be incorporated by soaking the dry material in aqueous solutions of these NO donors.[11] Alternatively, RSNOs can be chemically bonded to the material's structure *via* covalent linkages. Both approaches—physical absorption and covalent bonding—offer varying degrees of stability and provide distinct strategies to achieve controlled NO release, which can be fine-tuned for specific biomedical

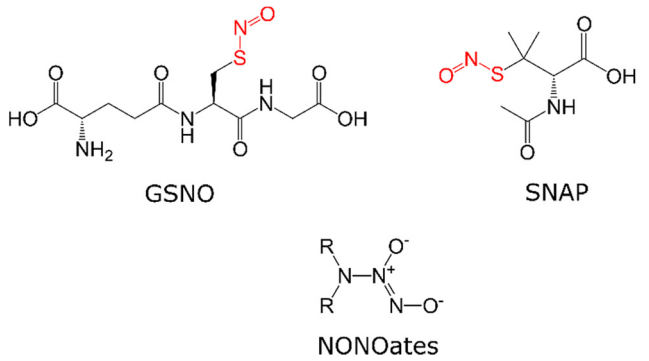

Fig. 1 Chemical structures of the NO donors most used in 3D printed NO releasing biomaterials: *S*-nitrosoglutathione (GSNO) *S*-nitroso-*N*-acetil-DL-penicilamine (SNAP), and amine-based-diazeniumdiolates (NONOates).

applications.[29,30] Fig. 1 shows the chemical structures of GSNO, SNAP and amine-based NONOates.

NO-releasing biomaterials

A variety of polymer-based systems and hydrogels have been investigated as matrices for creating NO-releasing biomaterials. For example, injectable hydrogels composed of poly(ethylene glycol) (PEG) and fibrinogen, combined with fibrin microparticles encapsulating SNAP, have been developed to form adhesive, NO-releasing hydrogels for tissue engineering.[31] Beyond PEG, other synthetic polymers have also been utilized, such as polyurethane. Notably, a composite of tryptophan-polyurethane and carboxylated polycaprolactone loaded with GSNO has been designed to promote antimicrobial and antibiofilm effects, specifically targeting wound healing applications.[32,33]

In addition, hydrogels for topical use have been explored, such as a LAPONITE®-polyamine composite loaded with NONOate, leveraging LAPONITE®'s natural gelling properties to deliver NO.[34] The versatility of NO-releasing biomaterials is further demonstrated by the development of antibacterial and conductive hydrogels, such as polyvinyl alcohol and sodium alginate (PVA-SA) hydrogels, also loaded with SNAP.[35] This wide range of material platforms highlights the potential of NO-releasing biomaterials for various therapeutic applications, from wound healing to tissue regeneration and antimicrobial treatments.

Natural polymers are increasingly being utilized in the development of NO-releasing biomaterials, offering promising applications in antimicrobial and wound healing therapies. Examples include biodegradable scaffolds composed of silk fibroin and zein protein, incorporating GSNO,[36] as well as alginate and calcium microspheres infused with SNAP.[37] Both approaches have demonstrated potent antimicrobial activity against *Staphylococcus aureus* and *Escherichia coli*. Furthermore, the antimicrobial efficacy of NO release has been confirmed using *in situ* ionotropically gelated SNAP-loaded calcium/alginate gels.[38] In addition to these, natural polymers can also be fabricated into sponge-like structures. For instance, gelatin sponges loaded with thiolated starch nanoparticles, which were subsequently *S*-nitrosated to create NO-releasing nanoparticles, have shown promise in wound dressing applications by enhancing cell attachment and promoting collagen production.[39] Another approach involves the functionalization of hyaluronic acid with NONOates to achieve controlled NO release, which has also demonstrated beneficial effects in wound healing. However, NONOate synthesis tends to be more complex and labor-intensive compared to RSNOs, making RSNOs a more practical and accessible choice for NO donor incorporation in biomaterials.

Our research group has explored the incorporation of RSNOs into different polymeric materials, including micellar Pluronic F127 thermogels, which enable controlled NO release either thermally or photochemically at targeted areas, particularly for topical applications. In these systems, the release profile of NO is regulated by the dimerization reaction of RSNOs located both in the hydrophilic poly(ethylene oxide) (PEO) corona of the micelles and in the intermicellar spaces.[40] Additionally, we developed *S*-nitrosothiol-functionalized polyvinyl alcohol (PVA) films blended with Pluronic (PVA-SNO/F127), which enhanced wound healing by promoting wound contraction and reducing the wound gap.[29,30] Recently, we advanced this work by creating photo-crosslinked chitosan cryogels functionalized with *S*-nitrosothioglycolic acid and *S*-nitrosomercaptosuccinic acid. These cryogels, designed for potential topical applications, demonstrated a high swelling capacity, allowing them to absorb wound exudate and deliver localized NO release to support wound healing.[41]

Despite the significant progress in developing NO-releasing materials, challenges remain, particularly regarding the structural complexity of the devices produced. The manual fabrication methods traditionally used for these materials are often labor-intensive, time-consuming, and difficult to reproduce, limiting their potential for more advanced biomedical applications. However, with the advent of 3D printing and additive manufacturing, the transition to more complex and reproducible NO-releasing devices has become both an inherent and inevitable step forward, offering new possibilities for innovation and application in the field.

Terminology of 3D-printed biomaterials

3D printing has emerged as a transformative technology in the biomedical field, enabling the precise fabrication of complex three-dimensional structures through layer-by-layer deposition, guided by computer-aided design (CAD) models. This technique facilitates the creation of highly customized devices, tissues, and organ constructs, offering significant potential for advancements in personalized medicine, tailored specifically to meet individual patient need.[42,43] However, the multidisciplinary nature of 3D printing in biomedicine involves experts

from various fields, including chemistry, bioengineering, pharmacy, biology, medicine, materials science, and computer programming. Consequently, the terminology used in different studies often varies depending on the background and preferences of the authors, leading to inconsistencies in definitions across the literature.[44–49] To address this variability, this section aims to provide standardized definitions of key terms related to 3D-printed biomaterials, based on a comprehensive review of the existing literature. This will promote clearer communication and understanding among researchers and practitioners in this rapidly evolving field.

Bioprinting terminology

Bioprinting. Bioprinting refers to the use of the additive manufacturing process to print 3D structures with biocompatible materials, which can be converted into tissues or organs by stimulating cellular activity. Constructs obtained by bioprinting can be used in regenerative medicine and in pharmacokinetic and cell biology studies.

Resolution. In 3D printing, resolution refers to the smallest feature size or the minimum dimensions that can be accurately produced by a given technique. Higher resolution allows for the creation of more intricate and detailed structures, which is crucial in applications like tissue engineering, where precision is essential.

Constructs. Constructs are the final 3D-printed objects or structures, created based on a CAD model. These are the physical representations of the digital design, produced through layer-by-layer printing processes.

Fidelity. Fidelity refers to how accurately the printed constructs match the dimensions and details of the original CAD model. Constructs that closely resemble the computational design are said to exhibit high fidelity.

Bioinks. Bioinks consist of living cells or cell aggregates, often combined with biocompatible materials such as hydrogels, biological substances, and active compounds. These bioinks are designed to support cell viability and biological function during and after the printing process.

Biomaterial Inks. In contrast to bioinks, biomaterial inks, are formulated without living cells. These inks provide greater versatility in printing processes and techniques. Biomaterial ink constructs are often used as scaffolds, designed to support subsequent cell proliferation and tissue development.

Printability. Printability refers to the ability of a bioink or biomaterial ink to be successfully printed, forming reproducible and structurally sound constructs. Printability is a key factor in ensuring the precision and functionality of 3D-printed biomaterials.

Post-processing. Post-processing (also referred as *postfabrication*) involves additional steps taken after the initial printing to enhance the integrity, structural stability of the construct or to add a functionality to the construct. Common post-processing methods include UV-visible curing, crosslinking in a bath, and other techniques that solidify or reinforce the printed material, ensuring it meets the desired mechanical and biological properties, while postfabrication may include the coating of the construct with one or more layers of other materials, the physical absorption of active principles and the chemical functionalization of the construct.

3D printing techniques for biomaterials

3D printing is categorized by the International Organization for Standardization (ISO) through the ISO/ASTM 52900 standard into seven processing categories. Among these, we found that two main categories are consistently used in research related to the 3Dprinting of NO-releasing biomaterials for biomedical applications: vat photopolymerization and material extrusion.

Vat polymerization

This category, which includes techniques like Stereolithography (SLA) and Digital Light Processing (DLP), is renowned for its high resolution. This process relies on four key components: a light source (a laser for SLA or a digital micromirror device (DMD) for DLP), a vat containing the 3D-printable inks, a light control system for selective photo-crosslinking, and a platform (moving along the *z*-axis) that anchors and supports the construct during printing.[50] These are photo-induced methods, where resins containing photoinitiators, monomers, and/or polymers undergo photopolymerization or photocrosslinking when exposed to electromagnetic radiation. The process enables the stepwise solidification of layers on a platform that incrementally moves along the *z*-axis, ultimately producing the final construct.[51] To replicate a CAD model, successive layers are cured and exposed to the light source, as shown schematically in Fig. 2a. One of the significant advantages of vat polymerization is its superior resolution, often reaching as fine as 20 μm – far surpassing that of extrusion-based methods. This makes it ideal for 3D printing intricate and complex structures. However, in biomedical applications, a major limitation is the availability of photoinitiators that are both water-soluble and biocompatible, making it challenging to incorporate these into bioinks that contain living cells or biological materials.[52,53] Despite these limitations, vat polymerization remains a powerful tool for creating high-

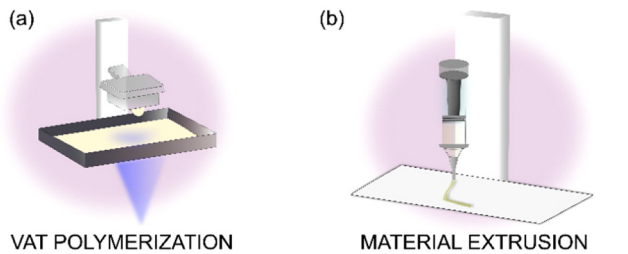

Fig. 2 Schematic drawings of the principal 3D printing categories used for the biomaterials development: (a) vat polymerization and (b) material extrusion.

resolution constructs, particularly in fields where precision and complexity are paramount.

Material extrusion

Material extrusion is the most used 3D printing technique for bioapplications due to its simplicity, accessibility, and cost-effectiveness. The process involves the use of a syringe connected to the printer, which extrudes material in continuous filaments through a nozzle, allowing for layer-by-layer deposition of the construct.[54] Fig. 2b provides a schematic illustration of the material extrusion process. Two primary extrusion-based approaches are frequently employed in the development of materials for biomedical applications:

Fused deposition modelling (FDM). In this method, melted polymers are extruded and deposited in layers according to a computer-aided design (CAD) model. The molten material is laid down on a build platform, where it solidifies and fuses with previous layers, gradually forming the desired structure.

Semi-solid extrusion (SSE). Unlike FDM, SSE is performed at lower temperatures and utilizes bioinks or biomaterial inks in the form of gels, pastes, or dispersions. This method, also known in the literature as hydrogel-forming extrusion or microextrusion, allows for the fabrication of constructs using biologically compatible materials without subjecting them to the high temperatures required in FDM.[55]

The resolution of constructs produced by extrusion-based methods is limited by the diameter of the nozzles, which dictates the thickness of the deposited filaments. Typically, extrusion-based printing achieves a resolution of around 100 μm, depending on the nozzle size used. Although this resolution is lower compared to other 3D printing techniques like vat polymerization, material extrusion remains a versatile and efficient method for fabricating bioengineered constructs.[56]

Printable biomaterials properties

Material selection is crucial in producing structures that closely replicate the unique properties and characteristics of biomedical devices, tissues, and grafts. As a result, the requirements for printable materials must account for factors such as biocompatibility, rheological behavior, structural integrity, and the final mechanical properties of the construct. Fig. 3 highlights these four key components in relation to printable materials for biomedical applications.

Rheological properties

The flow and viscosity characteristics of printable inks directly influence the 3D printing process. The rheological behavior of inks and printed structures is critical for ensuring printability, shape retention, and fidelity to the original 3D model.[57] Rheological parameters are specifically tailored for each printing technique. For instance, in the case of the SSE technique, low-viscosity inks make it difficult to form a stable, continuous filament, leading to reduced resolution as the filament spreads upon deposition. Conversely, high-viscosity inks can hinder material extrusion and may even cause nozzle clogging. Therefore, conducting rheological analyses is essential to determine the optimal viscosity range needed to achieve the desired pseudoplastic behavior in these fluids.[58] Typically, viscosity values reported in the literature range between 30 and 6 × 10^7 mPa s to prevent nozzle clogging.[59]

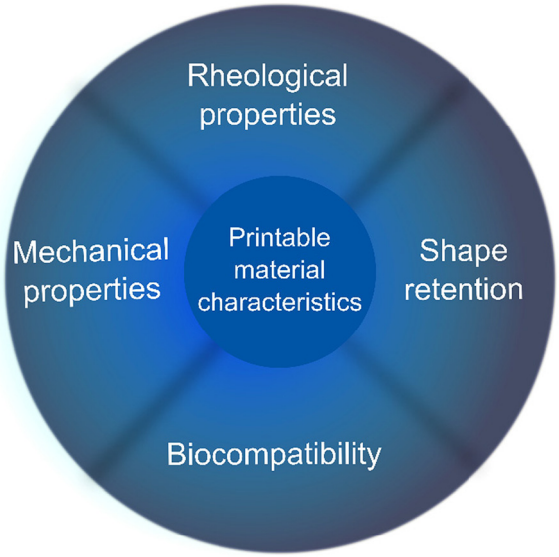

Fig. 3 Printable material characteristics in 3D printing for biomedical applications: rheological properties, shape retention, mechanical properties, and biocompatibility.

During the printing process, materials must exhibit fluidity with increasing shear rates, but once deposited, they must stabilize – a characteristic seen in shear-thinning materials. The successful formation of a continuous filament after extrusion depends on the viscoelastic nature of the fluid, which should display a predominantly elastic behavior at this stage. Furthermore, a short structural recovery time after extrusion is desirable to allow for optimal printability, indicating the material's ability to quickly restore its integrity.

In summary, the key rheological properties of printable inks include viscosity, viscoelastic shear modulus, and viscosity recovery. Viscosity governs the material's behavior both at rest and during flow, while shear-thinning behavior ensures effective extrusion and solid-like properties when at rest.[60] Additionally, the relationship between ink behavior, nozzle size, shape, and extrusion rate must be assessed to guarantee both printability and resolution.[61,62]

By contrast, vat polymerization requires inks with low-viscosity liquid behavior. The ink must flow through the vat to refill the area for subsequent light exposure as the print head lifts with each layer. In general, current research on vat polymerization inks does not emphasize detailed rheological characterization.[63] However, attention must be given to the longevity of inks used in vat polymerization, particularly regarding viscosity. When reusing photocurable inks, increased viscosity may result if the photopolymerization or

photo-crosslinking reaction extends beyond the construct. To minimize excessive light scattering, the use of photoblockers or photoinhibitors is often recommended. Additionally, filtration or sieving mechanisms can be employed to remove crosslinked aggregates, improving print quality.

Shape retention and fidelity

Another critical factor in 3D printing biomaterials is the need for post-processing, both during and after printing, to ensure the stability and shape retention of the printed structure in its solid form. This post-processing also guarantees accurate fidelity to the original 3D computer model. Generally, shape retention refers to the ink's ability to maintain its form and dimensions following extrusion and deposition, as well as after subsequent layers are added.[64] In photo-induced 3D printing, shape retention can be controlled by regulating photopolymerization and photo-crosslinking reactions. By applying spatial control of incident irradiation on the resin, it is possible to form layers with precise dimensions, thereby maintaining the dimensional fidelity of the final construct compared to the computational model.[65]

The structural stability of the printed construct is closely linked to crosslinking strategies, especially when using hydrogel matrices. Crosslinking can be induced by light or heat and can involve mechanisms that create chemical bonds or rely on physical and enzymatic interactions. Typically, polymer solutions undergo crosslinking either after the deposition of each layer or at the end of the printing process during extrusion. In this context, the constructs can be physically crosslinked by inducing gelation through thermal or ionic means, resulting in the formation of intermolecular forces that maintain the gel structure. Alternatively, chemical crosslinking can be used, where reagents promote covalent bonding between polymer chains to ensure the construct remains solid. In fused deposition modelling (FDM), structural stability is achieved by the solidification of melted polymer inks, particularly for scaffold production.[66]

Mechanical properties

The final construct of a printable biomaterial must possess sufficient mechanical strength to endure mechanical stress and deformation, particularly in applications involving organs and implants that are continuously subjected to mechanical forces in real biological environments. The crosslinking process, as discussed earlier, plays a significant role in determining the mechanical properties of the construct, as it helps achieve the desired mechanical characteristics for the specific application.[67] In the case of biomaterial inks composed of hydrogels, it is crucial to assess their swelling behavior. Hydrogels typically swell by allowing water to diffuse between the polymer chains. Unfortunately, many studies overlook this aspect and provide mechanical characterizations only in post-printing conditions. However, it is essential to evaluate the mechanical properties of the material under physiological conditions, where hydrogels will experience swelling.[68] This swelling process significantly affects the morphology of the entire gel and, consequently, its mechanical properties.[69]

Biocompatibility

Biocompatibility is a fundamental requirement for all biomedical materials. These materials must either support natural biological processes or intentionally induce specific biological effects. In essence, the components of these materials should be non-toxic and capable of integrating with target tissues, potentially promoting cellular adhesion, proliferation, and differentiation.[70] Biocompatible materials must also elicit a healthy immune response, even after implantation, and should be completely non-cytotoxic.[71] To meet these requirements, some devices are made from bioresorbable materials that fulfill their intended function and are then reabsorbed by the body over time.

In certain applications, biodegradability is crucial, as it allows the material to gradually degrade and be replaced by living tissue. This feature is particularly important when the material is used as a temporary scaffold for tissue regeneration, which will eventually be replaced by natural tissue. In such cases, the byproducts of the degradation process must also be non-toxic to cells.[72–74]

Integrating NO release with 3D-printed biomaterials

As discussed, incorporating NO release capabilities into 3D-printed biomaterials could enhance their therapeutic efficacy. This is based on the many beneficial effects demonstrated by NO-releasing biomaterials developed through other methods, such as solvent evaporation molding or medical device coatings. However, integrating 3D printing with NO release poses two significant challenges that need to be addressed:

1. Thermal sensitivity. Molecules or chemical groups that release NO, such as RSNOs and NONOates, are thermally sensitive. When incorporated into a resin for FDM-based 3D printing, they undergo thermal decomposition during the extrusion process. As a result, 3D printing of NO-releasing biomaterials by extrusion has so far been limited to cold extrusion of hydrogels, which undergo cross-linking *via* mechanisms like ionotropic cross-linking. In this context, printing hydrogel constructs using the FRESH (Freeform Reversible Embedding of Suspended Hydrogels) technique emerges as a promising alternative.[75]

2. Photosensitivity. RSNOs, NONOates, and other NO donors, such as sodium nitroprusside (SNP), Roussin's Red and Black Salts, and ruthenium nitrosyl complexes, are photosensitive. They release NO through photochemical reactions triggered by visible or ultraviolet light.[76,77] This characteristic complicates or limits their application in 3D printing processes like stereolithography (SLA) or digital light processing (DLP).

The following subsections describe key strategies developed to overcome these challenges, making it possible to integrate

Table 1 Summary of the materials, NO donor, 3D printing category and nitric oxide releasing strategy used in the 3D printing of NO-releasing biomaterials

Materials[a]	NO donor	3D printing category	Nitric oxide releasing strategy	Ref.
Gelatine-alginate	SNAP	Extrusion	Cold extrusion of SNAP-charged hydrogel	79
PLA coated with PEG, PCL, and PEG-PCL	SNAP	FDM	Postfabrication coating	18, 82 and 84
Mesoporous Silica@MXene	SNO-funtionalized silica	Extrusion	Postfabrication impregnation	87
Methacrylated poly(dodecanediol citrate)	SNAP	DLP	Postfabrication absorption from SNAP solution	88
Polycarbonate urethane-silicone (PCU-Sil)	SNAP	FDM	Postfabrication absorption from SNAP solution	83
Methacrylated poly(dodecanediolcitrate-*co*-dodecanediol mercaptosuccinate) mP(DC-*co*-DM)	mP(DC-*co*-DMSNO)	DLP	Postfabrication functionalization of the scaffold	89
PAA/F127/CNC	GSNO	DLP	Postfabrication absorption from GSNO solution	90
Silicone elastomers of (PDMS)	SNAP and GSNO	SSE	Dispersion of solid NO donor particles in the ink	92

[a] For the chemical structures of the polymers used in the materials (except those in ref. 82 and 86) see Table S1 (ESI†).

3D printing with externally controlled NO release. The main strategies are summarized in Table 1.

(a) Cold extrusion of SNAP-charged hydrogel. NO plays a vital role in signaling processes related to wound healing, including vascular homeostasis, inflammation regulation, and antimicrobial action.[78] With the aim of accelerating wound healing through topical NO delivery, Wu *et al.*[79] developed a bioink tailored for 3D bioprinting, specifically for creating scaffolds to treat severe burns. Their bioink formulation combined sodium alginate, gelatin, SNAP, and Adipose-Derived Mesenchymal Stem Cells (ADSCs) for extrusion-based 3D printing. This approach led to significant improvements in cell migration, angiogenesis, and the growth of Human Umbilical Vein Endothelial Cells (HUVECs) *in vitro*. In addition to these *in vitro* results, the study also demonstrated accelerated wound healing over 14 days in a mouse model, attributed to the bioink's ability to stimulate epithelialization and collagen production. Immunohistochemistry assays further revealed that the 3D-printed system contributed to the regulation of vascular endothelial growth factor (VEGF), a critical factor in the neovascularization process. While the study showcases the potential of SNAP-loaded hydrogels for 3D bioprinting, it's important to note that SNAP was incorporated into the hydrogel within the printer syringe, and the printed constructs were immediately immersed in a calcium chloride solution for crosslinking. Despite SNAP's stability in its solid form, its inclusion in the aqueous medium of gelatin and alginate initiates its decomposition, resulting in NO release. This decomposition continues during the extrusion printing process and throughout the subsequent immersion in the $CaCl_2$ solution for crosslinking. This ongoing decomposition of SNAP in the aqueous environment introduces two major challenges: 1 – Uncertainty in SNAP concentration: The exact SNAP concentration present in the construct immediately before application is unknown, as some of the SNAP is lost during printing and crosslinking. 2 – Lack of storage feasibility: The constructs cannot be stored in a hydrated form and must be prepared extemporaneously, just before application.

This limitation may pose challenges in practical, real-world scenarios. One possible strategy to partially overcome these difficulties is to freeze the construct immediately after printing, followed by freeze-drying. In this way, as has already been demonstrated in studies by Póvoa *et al.*,[80] the preservation of the RSNO in the dried construct can be ensured and it can therefore be stored in a stable form for long periods of time. In this case, for application, the construct can be hydrated immediately before use or applied in dry form to the lesion to be hydrated through the absorption of exudate (in the case of moist lesions). Most dry hydrogels swell rapidly after contact with an aqueous medium and the absorption of water will promote the mobilization of RSNO molecules and their dimerization with the release of NO, as already reported in a similar strategy for hydrogels loaded with GSNO.[17]

(b) Postfabrication coating with NO-releasing polymer layers. Implantable blood-contact devices require specific attributes for effective biological applications, such as promoting endothelialization and ensuring hemocompatibility. NO plays a crucial role in these devices by exerting antithrombogenic action.[81] To reduce the thrombogenicity of small-diameter vascular grafts (SDVGs), Kabirian *et al.*[18,82] developed a method using FDM 3D printing with polylactic acid (PLA) filaments. The grafts were fabricated by extruding PLA through a needle at 220 °C. However, SNAP, which was used as a nitric oxide donor, could not be pre-incorporated into the PLA filament due to its thermal sensitivity, which would cause decomposition during extrusion. To circumvent this issue, these researchers coated the PLA constructs with poly(ethylene glycol) (PEG), polycaprolactone (PCL), or a PEG/PCL blend containing SNAP. This coating was achieved by immersing the PLA constructs in polymeric solutions of PEG, PCL, or PEG/

PCL containing SNAP in tetrahydrofuran (THF), followed by solvent evaporation. To further reduce the rate of NO release, an additional top coating (tc) of PCL was applied over the coated constructs. The process is illustrated in Fig. 4a. The coated tubular constructs were tested for their ability to inhibit platelet aggregation by incubating the PLA constructs coated with PEG-PCL-SNAP-tc in human platelet-rich plasma (PRP). Control PLA constructs coated with PEG-PCL-tc were also incubated under the same conditions. The results, shown in Fig. 4b, revealed that the NO-releasing constructs strongly inhibited platelet aggregation. Scanning electron microscopy (SEM) images (Fig. 4c and d) demonstrated the difference in platelet morphology. In the absence of NO (PEG-PCL-tc), activated platelets with irregular shapes and protruding pseudopods were observed. In contrast, in the presence of NO (PEG-PCL-SNAP-tc), the platelets exhibited a non-activated, spherical morphology. In summary, the SNAP-coated vascular grafts effectively inhibited platelet aggregation for a significant 14-day period, successfully preventing thrombus formation within the grafts. In a subsequent study, Kabirian *et al.*[83] developed SDVGs using PCL and an innovative method to incorporate SNAP into the device. In this approach, SNAP was encapsulated within multi-walled carbon nanotubes (MWCNTs), which were dispersed in a blend of poly(ethylene glycol) (PEG) and PCL. This blend was then incorporated into the printed constructs through a coating process. A schematic of the preparation of NO-releasing SDVGs is shown in Fig. 5a.

Encapsulating SNAP within the carbon nanotubes resulted in a prolonged release of NO, extending up to 18 days. This system demonstrated good cytocompatibility, enhanced the proliferation of endothelial cells, and exhibited antimicrobial activity *in vitro*. Immunofluorescence and MTT absorbance assays (Fig. 5b and c) were conducted with endothelial cells incubated with the NO-releasing graft, a control graft, and culture medium after 7 days. The MTT assay showed that NO release from the grafts significantly enhanced cell proliferation. The morphology of human umbilical vein endothelial cells (HUVECs) was also assessed. Images revealed that cells in both NO-releasing and control constructs displayed a spread-out morphology, indicating favorable conditions for cell growth. Furthermore, as shown in Fig. 5e, the NO-releasing constructs accelerated endothelial cell migration from the

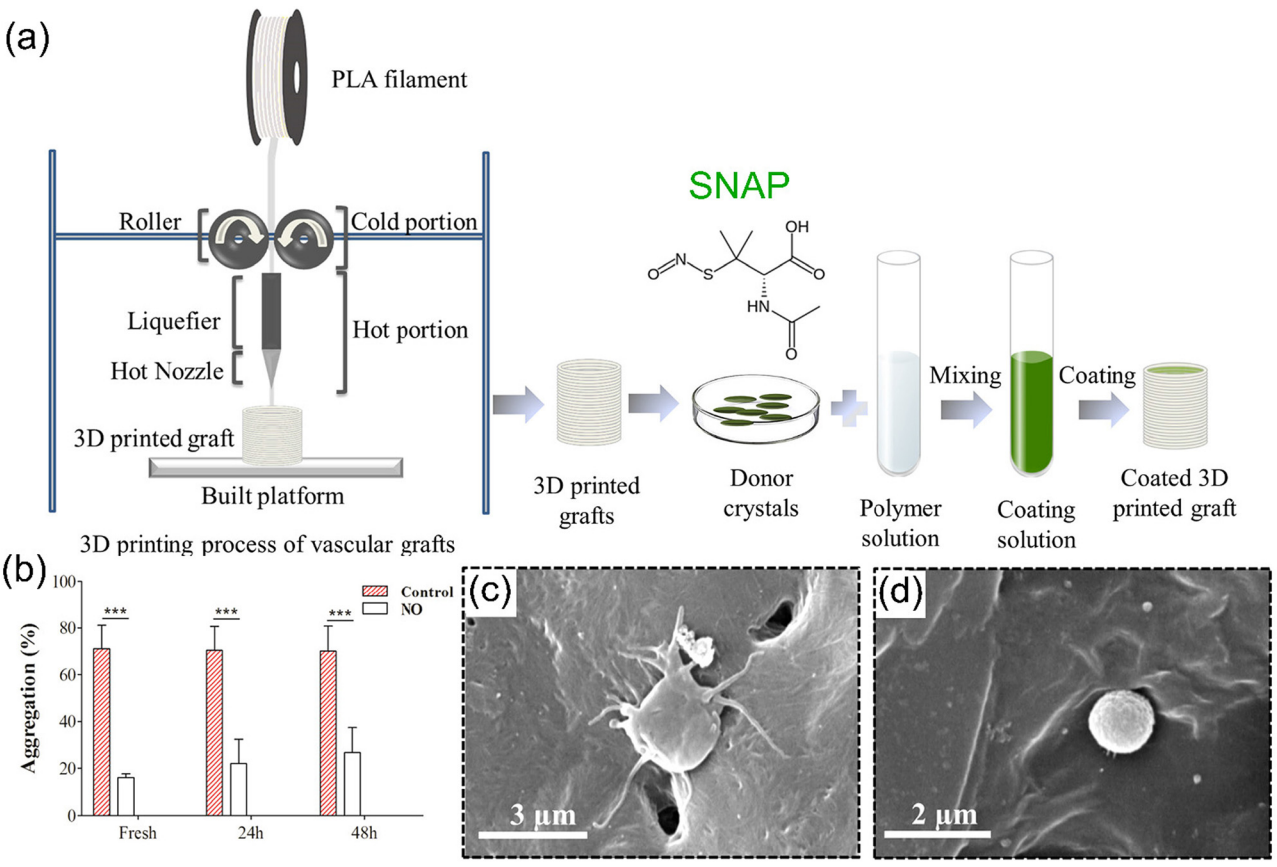

Fig. 4 (a) Schematic representation of NO-releasing vascular graft printing using PLA filament with the final SNAP solution coating in polymer. (b) Aggregation (%) of fresh human platelet rich plasma (PRP) of three donors incubated with fresh, 24 h, and 48 h pre-soaked grafts for 10 min. Morphology of graft-adhered platelets after 1 h incubation of fresh human PRP with (c) PEG-PCL-tc coated control grafts and (d) PEG-PCL-SNAP-tc coated grafts showing irregular morphology with protruded pseudopodia and resting spherical morphology, respectively. Reprinted (adapted) with permission of F. Kabirian, B. Ditkowski, A. Zamanian, M. F. Hoylaerts, M. Mozafari and R. Heying, *ACS Biomater. Sci. Eng.*, 2019, **5**, 2284–2296. Copyright 2019, American Chemical Society.

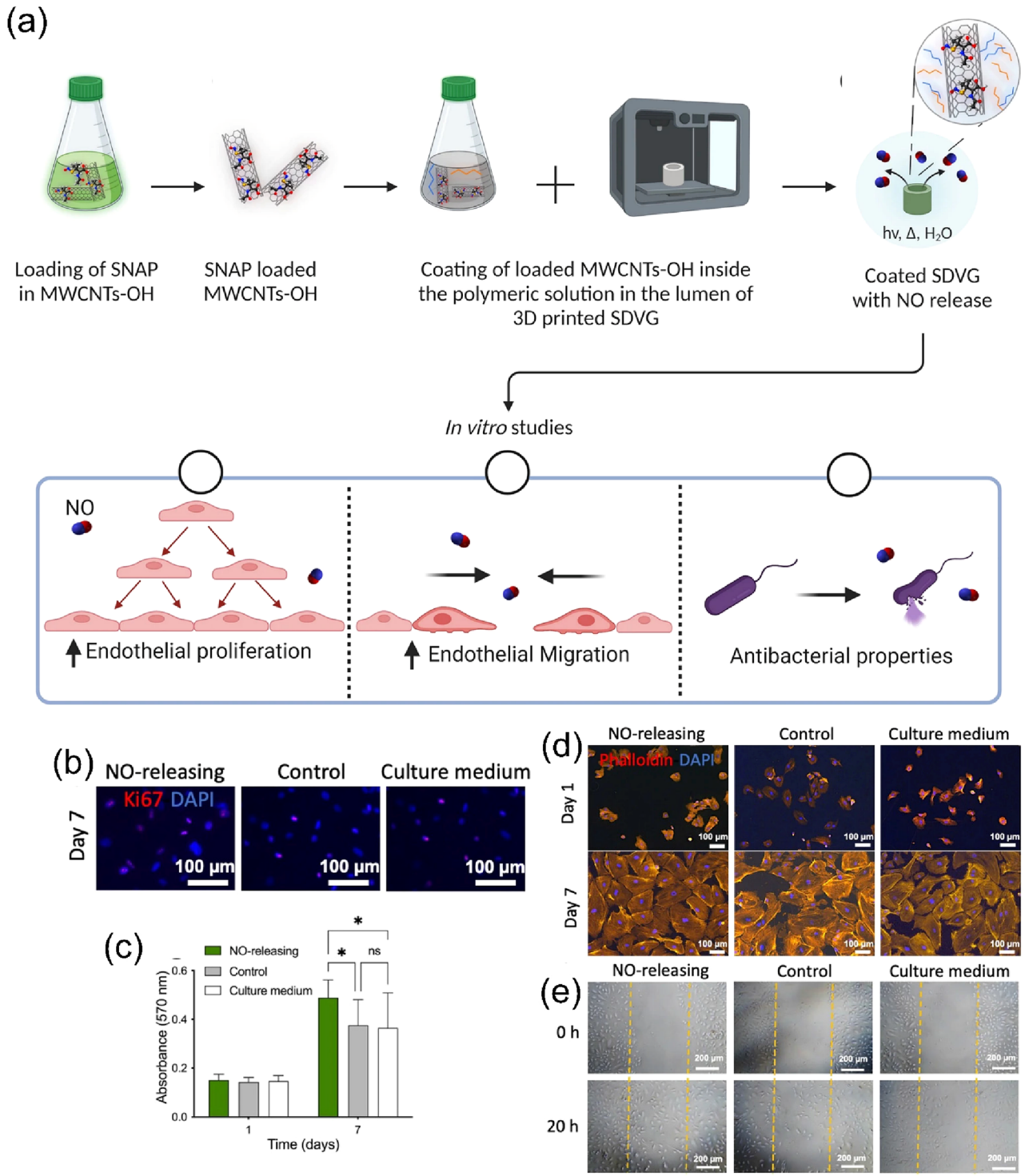

Fig. 5 (a) Preparation of NO-releasing vascular grafts (SDVGs) and *in vitro* biological effects. The upper part depicts the loading of SNAP into hydroxyl-terminated multi-walled carbon nanotubes (MWCNTs-OH), coating them within the lumen of 3D-printed SDVG, and subsequent NO release. The lower part highlights the graft's biological properties, including enhanced endothelial cell proliferation, migration, and antibacterial activity. (b) Immunofluorescence: ECs incubated with NO releasing graft, control graft and culture medium after 7 days. (c) absorbances by MTT assay. (d) Immunofluorescence imaging of HUVECs after 1 and 7 days of cultivation in direct contact with NO-releasing grafts, control grafts and culture medium (e) Scratch assay of HUVECs in presence of NO-releasing graft, control graft and culture medium. Reprinted (adapted) with permission from F. Kabirian, P. Baatsen, M. Smet, A. Shavandi, P. Mela and R. Heying, *Sci. Rep.*, 2023, **13**, 1–12. Copyright © 2023.

neighboring vessel toward the wounded site of the graft. While these studies produced promising results, it is important to note that the coating strategy used in both cases is not exclusive to constructs obtained by 3D printing. This method can be applied to constructs produced using various other manufacturing techniques.

With a similar goal, Chug *et al.*[84] created a polycarbonate urethane-silicone (PCU-Sil) for the fabrication of medical devices through additive manufacturing *via* extrusion. The devices were manufactured in the form of discs with varying porosities to assess the effect on NO release from the materials impregnated with SNAP solution. The authors observed that different porosities exhibited distinct NO release profiles varying from 7 to 14 days, thereby leading to differences in antimicrobial action against *Staphylococcus aureus*. *In vitro* assays conducted during 24 h resulted in over 99% bacterial death. Through this study, the authors successfully employed a polycarbonate-based silicone elastomer biomaterial for NO release with potential antimicrobial action for the first time, which may be utilized in the future for the manufacturing of medical devices.

(c) Postfabrication impregnation of porous 3D-printed scaffold. NO has been extensively studied in bone tissue repair due to its significant role in regulating inflammation, angiogenesis, and osteogenesis.[85] Low concentrations of NO are known to stimulate osteoblast growth and differentiation, making it an attractive agent for bone tissue engineering.[86] The use of 3D-printed scaffolds loaded with NO donors presents a promising approach in this field. Yang *et al.*[87] developed a bioglass scaffold using 3D printing, employing the SSE technique for controlled NO release, with a focus on applications in bone regeneration and osteosarcoma treatment. Their approach involved creating an inorganic biomaterial consisting of mesoporous silica (MS)-coated 2D Nb_2C MXene, loaded with *S*-nitrosothiol (SNO) groups as NO donors, which were incorporated into the large macropores of a 3D-printed bioglass scaffold (BG). This system, denoted as MS/MXene-BG-SNO (abbreviated as MBS), combines the advantages of NO release with a bioactive scaffold for bone repair. To fabricate this construct, the researchers first functionalized MS with thiol groups (SH) using mercaptosilane modification, followed by *S*-nitrosation to form pendant SNO moieties. The MXene and SNO-functionalized MS were then impregnated into the pre-printed scaffolds. The resulting device exhibited photothermal characteristics, which were activated by exposure to near-infrared radiation (NIR). Upon NIR exposure, the scaffold released phosphate, calcium, and NO, while locally raising the temperature to 60 °C. This localized temperature increase facilitated the ablation of bone cancer cells, providing a burst of NO release in both *in vitro* and *in vivo* studies using ectopic osteosarcoma and cranial defect models in mice. The study also reported excellent adhesion and viability of human bone mesenchymal stem cells (hBMSCs) on the scaffold's surface, promoting osseointegration. This research represents a significant advancement in the treatment of osteosarcoma through the integration of photothermal therapy and NO release.

In this approach, the porous bioglass scaffold was obtained using 3D printing, while the NO-releasing properties were introduced later by impregnating the pores with mesoporous silica functionalized with NO-donating SNO groups. This strategy is similar to the previously mentioned method of coating constructs with NO-donor materials. It can, in principle, be used to impregnate porous materials produced by other manufacturing techniques beyond 3D printing.

(d) Postfabrication absorption of SNAP from ethanolic solution. The study reported by de Oliveira *et al.*[88] describing the manufacture of NO-releasing vascular stents illustrates the strategy of post-printing incorporation of a NO donor into the constructs by absorption from solution. This study focuses on the development of bioresorbable vascular stents using the DLP 3D printing technology. The stents were made from methacrylated poly(dodecanediol citrate) (mPDC), a photocrosslinkable, bioresorbable polyester. After the DLP printing process, the stents were impregnated with SNAP, by absorbing it from an ethanolic solution. The method of SNAP incorporation represented a significant advancement because it allowed homogeneous loading of SNAP across both the surface and bulk of the stents. This uniform distribution ensured that the SNAP-loaded constructs remained stable after solvent removal, allowing for long-term storage. Additionally, these stents demonstrated a prolonged, controlled release of NO, which is regulated by the hydration and hydrolysis rates of the stent material upon contact with an aqueous environment. The slow, sustained release of NO makes these 3D-printed stents particularly promising for use as intracoronary stents, where NO's antithrombogenic and antiplatelet properties can help prevent restenosis and late thrombosis. The controlled release of NO from the luminal surface of the stents may provide therapeutic benefits, addressing common complications associated with stenting, such as thrombosis and impaired endothelial healing. The strategy allowed the production of 180 BVS per print pointing to a simple and scalable method to produce BVS.

(e) Postfabrication functionalization of the scaffold. Similar to the previous example, a study by de Oliveira MF *et al.*[89] also utilized DLP 3D printing to fabricate bioresorbable vascular stents, this time using a novel photocurable copolyester, methacrylated poly(dodecanediol citrate-*co*-dodecanediol mercaptosuccinate) (mP(DC-*co*-DM)). The key innovation in this study was the incorporation of NO donors, specifically RSNO groups, which were chemically bonded to the polymer chains of the copolymer, enabling a controlled release of NO. Notably, the –SNO moieties were generated in a post-printing step through an *S*-nitrosation reaction. The stents were first fabricated using DLP technology, ensuring high fidelity and precision in their design. Fig. 6a and b illustrate two stent models, A and B, while Fig. 6c provides images of the 3D-printed stents, each with a diameter of 5 mm. After printing, the stents underwent chemical modification: the free sulfhydryl groups on the polymer backbone were converted into *S*-nitrosothiols by immersing the stents in a 0.1 M butyl nitrite ethanolic solution for 4 h at room temperature, protected from

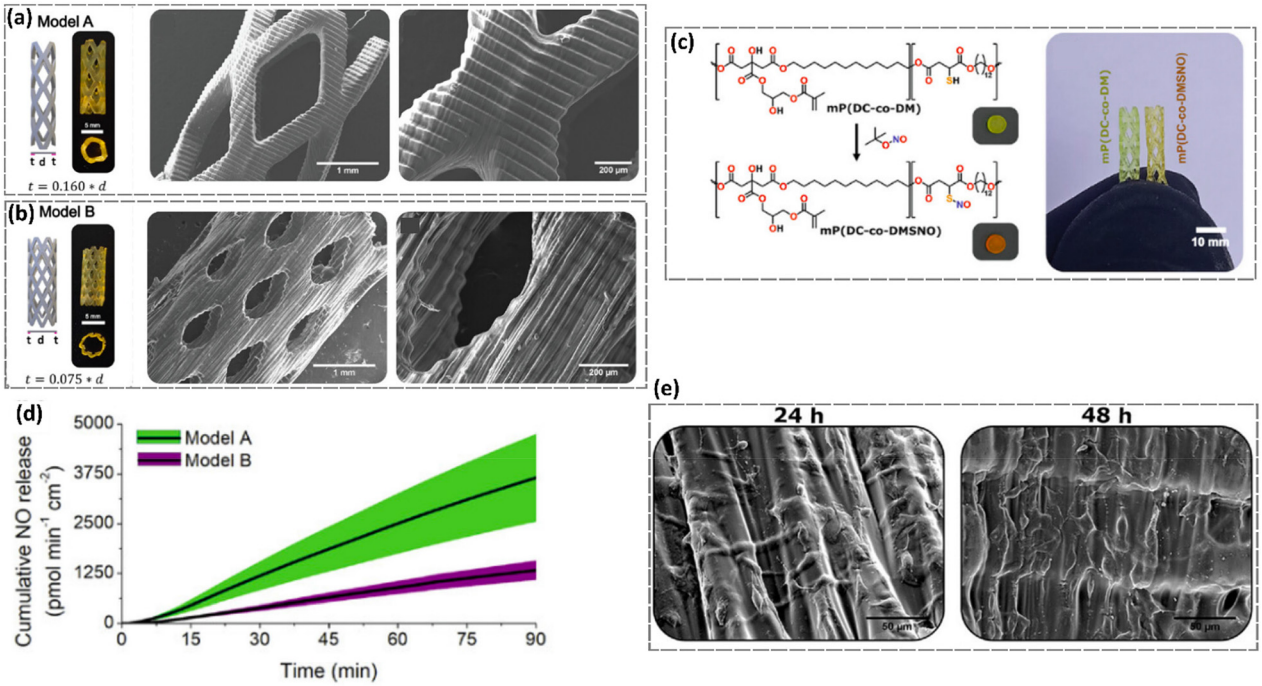

Fig. 6 (a, b) CAD model, macroscopic pictures and scanning electron micrographs of 3D printed 5 mm diameter mP(DC-*co*-DM)5 stents, models A and B. (c) Scheme of the *S*-nitrosation reaction of mP(DC-*co*-DM) to produce mP(DC-*co*-DMSNO), and photographs of model A mP(DC-*co*-DM)5 and mP(DC-*co*-DMSNO)5 stents, highlighting the colour change after the *S*-nitrosation reaction. (d) Cumulative NO release curves of model A and B mP(DC-*co*-DMSNO)5 stents during the first 60 min after immersion in water at 37 °C. (e) Scanning electron micrographs of the luminal surface of mP(DC-*co*-DMSNO)1 model A stent coated with endothelial cells after 24 and 48 h incubation. Reprinted (adapted) with permission from M. F. de Oliveira, L. C. E. da Silva, D. M. Catori, M. V. Lorevice, K. E. A. Galvão, A. L. G. Millás and M. G. de Oliveira, *Macromol. Biosci.*, 2023, **23**, 2200448. Copyright 2023.

light. This postfabrication process ensured that NO-releasing *S*-nitrosothiol groups were evenly distributed both on the surface and within the bulk of the stent, allowing for a sustained and controlled NO release. Fig. 6d shows the cumulative NO release profile of the mP(DC-*co*-DMSNO) stents during the first hour after immersion in water at 37 °C.

The results indicated that NO release from the stents was controlled by the hydration and hydrolysis of the polymer when in contact with an aqueous medium. This controlled release profile is highly advantageous for vascular stents, as the NO's antiplatelet and antithrombogenic properties help prevent restenosis and thrombosis. Furthermore, the study demonstrated that by adjusting the composition of the copolyester and the stent's geometry, the rate of NO release can be modulated, making this a promising approach for bioresorbable vascular stents. Preliminary biological assays in cell culture showed successful endothelial cell adhesion to the stent surface, with NO release aiding in their endothelialization. Fig. 6e shows scanning electron microscopy (SEM) images of the luminal surface of mP(DC-*co*-DMSNO)1 model A stents, with endothelial cells spread across the surface after 24 and 48 h.

(f) Postfabrication absorption of GSNO from solution. Santos *et al.*[90] described the fabrication of NO-releasing semi-interpenetrating networks of poly(acrylic acid)/Pluronic F127/cellulose nanocrystals using the DLP 3D printing. In this study, high-fidelity 3D constructs which were subsequently dried by lyophilization and charged with GSNO through absorption from aqueous GSNO solutions and dried again by lyophilization. As a result, this postfabrication approach allowed the preparation of stable GSNO-charged constructs. By using different GSNO concentrations, different levels of GSNO load were obtained leading to different rates of thermal NO release triggered by the rehydration of the dry constructs. Fig. 7a shows a scheme of the 3D printing and GSNO charging steps. The printing fidelity and resolution of the construct is shown in the SEM micrographies of Fig. 7b–d. In addition, Fig. 7e shows that the NO release kinetics which exhibited a dose-dependent behavior with respect to the GSNO loading characterized by rapid initial NO release steps within the first hour, followed by a plateau of nearly constant rates of NO release. This new approach stands out for its 3D printing of high-resolution hydrogel constructs using the DLP technique and the possibility of storing the GSNO-loaded constructs in a stable form. It can therefore be extended to other hydrogels that can be printed not only by DLP, but also by extrusion, and is a promising strategy for the development of customized NO-releasing 3D-printned hydrogel devices.

(g) Dispersion of solid NO donor particles in the ink. As stated previously, the biological activity mediated by NO

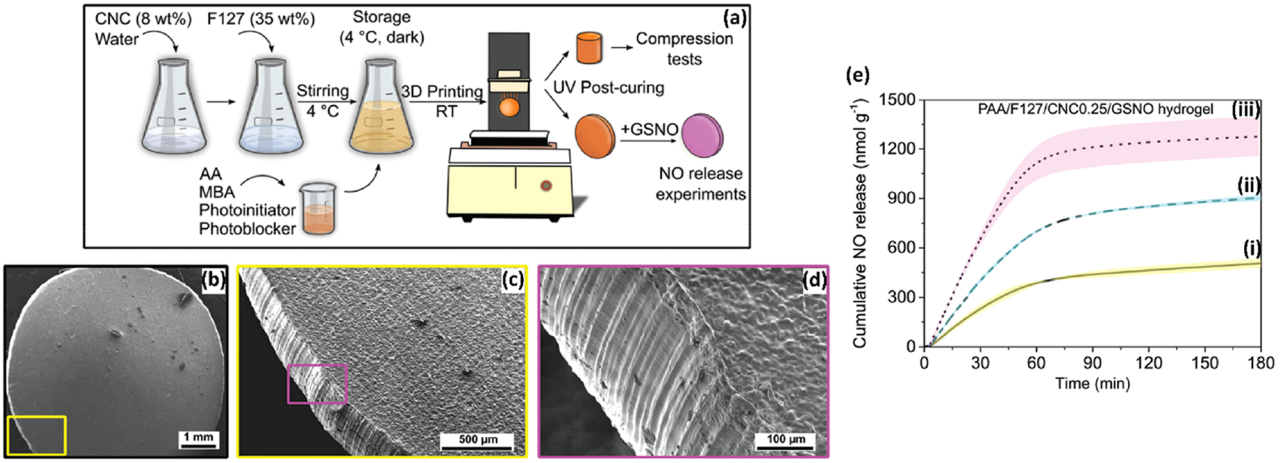

Fig. 7 (a) Scheme of the preparation of 3D printable hydrogel ink comprised of poly(acrylic acid) (PAA), Pluronic F127 micelles (F127), and cellulose nanocrystals (CNC) for DLP 3D printing, followed by *S*-nitrosoglutathione (GSNO) charging through absorption from solution. (b–d) Representative scanning electron micrographs with increasing magnifications of the surface of 3D-printed PAA/F127/CNC0.25/GSNO hydrogel disks. (e) Real-time NO release from 3D-printed PAA/F127/CNC0.25/GSNO hydrogel discs loaded with GSNO solutions (i) 5 mM, (ii) 10 mM, and (iii) 20 mM. Reprinted (adapted) with permission from M. I. Santos, L. C. E. da Silva, M. P. Bomediano, D. M. Catori, M. C. Gonçalves and M. G. de Oliveira, *Soft Matter*, 2021, **17**, 6352–6361. Copyright 2021.

within the organism is dependent on its concentration range, and at elevated concentrations, NO exhibits antibacterial effects due to the generation of reactive nitrogen species, leading to bacterial death.[91] Li *et al.*[92] reported a one-step 3D printing strategy to create drug-eluting polymer devices with a drug-loaded bulk and a drug-free coating by extrusion 3D printing utilizing a silicone ink infused with NO donors to fabricate devices with antimicrobial properties. In this approach, the authors circumvented the impediment of using the extrusion technique based on FDM extrusion (which leads to thermal decomposition of the NO donor), by using a high-viscosity liquid silicone resin, which can be cold-extruded and quickly vulcanized after exposure to ambient humidity. The strategy also avoids the need for irradiation in the DLP technique, which leads to the photodecomposition of the NO donors. However, it is important to note that the NO donors used in this study, GSNO and SNAP, were incorporated into the resin in the form of micronized crystals. It comprises therefore a dispersion of crystals leading to a two-phase resin. Micrographs showed inhomogeneous segregation of the crystals on the surface of the constructs, which was partly overcome by coating the constructs with a layer of pure silicone.

The researchers fabricated specimens in a tubular form and observed the sustained stability of both NO donors throughout the printing process, with the crystals effectively preserved within the printed constructs. Fig. 8a and b show the NO release profile of the SNAP-doped silicone rubber tube with PDMS construct in PBS at 37 °C and a picture of the construct.

The constructs obtained showed NO release over 7 days immersed in PBS solution at 37 °C with decreasing NO fluxes in the range of 3.8×10^{-10} mol min^{-1} cm^2 to 0.5×10^{-10} mol min^{-1} cm^2. As GSNO or SNAP crystals do not release NO

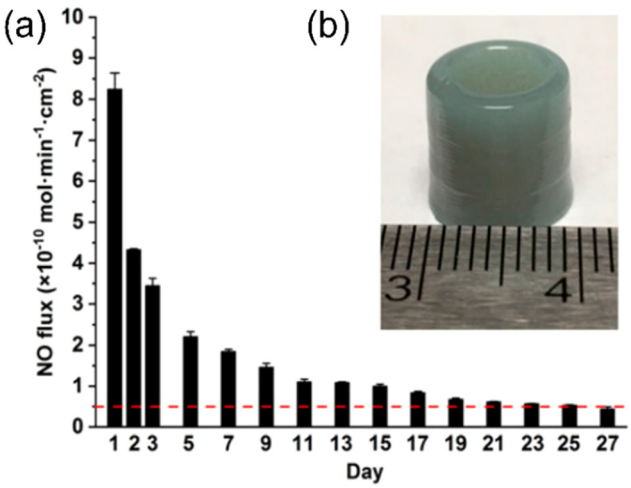

Fig. 8 (a) NO release from SNAP-doped silicone rubber tube with PDMS construct in PBS solution at 37 °C. (b) Picture of the 3D-printed SNAP-loaded construct with PDMS coating. Reprinted (adapted) with permission from W. Li, Y. Yang, C. J. Ehrhardt, N. Lewinski, D. Gascoyne, G. Lucas, H. Zhao and X. Wang, *ACS Appl. Bio Mater.*, 2021, **4**, 7653–7662. Copyright 2021.

directly, the release of NO was attributed to the slow dissolution of the crystals by the water absorbed by the constructs when immersed in PBS solution. It was observed that the NO released by the devices inhibited the bacteria biofilms formation of *Proteus mirabilis* in an *in vitro* model, during 24 h. Besides, the SNAP-printed construct promoted good cell viability, suggesting a potential alternative for preventing urinary catheter infections.

Future perspectives

Although the photochemical release of NO from RSNOs can be used as a tool to trigger the release of NO from an external stimulus,[93] the photosensitivity of RSNOs limits their use in the DLP 3D printing technique. In this case, the photochemical release of NO during the printing process not only consumes part of the RSNO stock, but the NO released also reacts with the radical species, blocking the radical propagation that leads to the photocrosslinking of the resin, impairing the printing process itself. One promising approach to overcome this limitation is the incorporation of RSNOs into polymeric nanoparticles, enabling the development of NO-releasing inks for a one-step printing process. Catori *et al.*[94] have recently shown that integrating PLGA nanoparticles (NPs) functionalized with GSNO into *in situ* photocrosslinkable hydrogels effectively protected GSNO from photodecomposition, allowing for sustained NO release at rates capable of promoting cell proliferation. Additionally, encapsulating GSNO in the NPs prevented the partial inactivation of radical species formed by photoinitiator homolysis, which occurs when GSNO is free in solution. As a result, the gelation time for hydrogels with and without NPs remained consistent. This work opens the possibility of developing inks with direct inclusion of RSNOs, suitable for both material extrusion and vat polymerization techniques.

Another avenue worth exploring is the incorporation of NO donors into bioinks. The potential of bioinks for 3D printing NO-releasing biomaterials remains largely underexplored in the current literature. Incorporating NO donors into bioinks could mitigate cytotoxic effects while enhancing biocompatibility. Given NO's crucial role in cellular signaling and tissue regeneration, it is an attractive candidate for improving the compatibility of 3D-printed biomaterials with living systems. In photoassisted 3D printing, the requirement for photoreactive substances, photoinitiators, and photoblockers—some of which exhibit cytotoxicity—limits the inclusion of cells within the ink.[95] Conversely, extrusion printing may present challenges related to shearing forces that could also limit bioink applications.[96] Nevertheless, NO could potentially improve biocompatibility and promote cell proliferation in both cases, representing a promising pathway for future research.

Researchers are also actively exploring new biocompatible materials and 3D printing strategies to address broader challenges such as the vascularization of printed organs, the reproduction of physiological organ functions, and the mimicking of tissue architecture. Insufficient or immature vascularization in implanted constructs can lead to oxygen and nutrient deprivation, resulting in low cell viability and organ malfunction. Recent efforts to overcome this limitation have focused on incorporating pro-angiogenic factors into ink formulations and pre-vascularizing constructs *in vitro* or *in vivo* using endothelial cells.[97,98] However, it is not unreasonable to consider the angiogenic properties of NO to develop bioinks capable of inducing vascularization in printed organs and tissues. These innovative approaches not only address current limitations but may also pave the way for new advancements in tissue engineering and regenerative medicine.

Concluding remarks

Integrating NO release with the 3D printing of biomaterials offers several potential benefits, including enhanced tissue integration and improved biocompatibility of implants. NO may promote cell adhesion and proliferation on the surface of 3D-printed biomaterials, supporting, for example, the growth of osteoblasts in bone fixation plates or pins, chondrocytes in intra-articular cartilage replacement prostheses, and endothelial cells in vascular prostheses. Additionally, NO release may effectively inhibit platelet adhesion, reducing the risk of thrombus formation in intracoronary stents and endovascular catheters. Furthermore, in all types of implantable scaffolds, controlled NO release may exert strong antibacterial action, significantly lowering the likelihood of hospital-acquired infections.

The techniques developed so far enable the incorporation of NO donors into biomaterials produced by 3D printing, both through extrusion and DLP methods. However, significant challenges remain in both approaches. In hot extrusion techniques, such as FDM or SSE, the thermal decomposition of NO donors continues to be an issue, while in DLP printing, the photochemical decomposition of NO donors, such as GSNO and SNAP, as well as NONOates, which are both thermo- and photosensitive, limits their applicability. Cold extrusion printing of hydrogels containing NO donors, followed by crosslinking *via* ionotropic complexation, has the potential to avoid thermal degradation of the NO donors. However, this strategy requires the immediate stabilization of the constructs through freezing and lyophilization, or their immediate use. Alternatively, different post-fabrication coating techniques, involving layers containing NO donors, can be employed. While this approach adds extra steps to the manufacturing process and limits the loading of NO donors to the surface of the constructs or to pore filling, it provides a viable option for modulating NO release at specific sites. Other postfabrication strategies, such as the incorporation of NO donors throughout the entire construct by absorption from aqueous or organic solutions, have also shown promise. Although these methods require additional steps (absorption and solvent removal), they can ensure prolonged NO release, governed both by water absorption and the hydrolytic degradation of biodegradable constructs, such as polyesters. Additionally, functionalization of polymer chains with NO donor groups, such as the *S*-nitrosation of thiolated polymers to form polynitrosated polymers, allows for the efficient loading of –SNO groups both on the surface and within the bulk of the constructs. The only reported strategy to date that enables the direct incorporation of NO donors into resin is based on the dispersion of solid NO donor crystals within the resin. However, this approach still faces the challenge of achieving homogeneous crystal dispersion to control NO release rates more precisely. A promising

strategy involves encapsulating NO donors in micro- or nanoparticles that protect them from radical reactions during 3D DLP printing, promoting controlled NO release triggered by the hydration of the construct. This approach could offer a solution to integrate NO release in a single 3D printing step, representing a promising avenue for the development of 3D-printed NO-releasing biomaterials. In conclusion, although significant progress has been made, challenges remain in optimizing the controlled incorporation and release of NO in 3D-printed biomaterials. Continued development of new techniques and exploration of innovative strategies will further push the boundaries of this emerging field, with the potential to profoundly impact regenerative medicine, medical devices, and other biomedical applications.

Author contributions

H. V. A.: conceptualization, writing – original draft; writing – review & editing; M. P. B.: conceptualization, visualization, writing – original draft; writing – review & editing; D. M. C.: writing – original draft; writing – review & editing; E. H. C. S.: writing – original draft; writing – review & editing; and M. G. O.: funding acquisition, project administration; supervision; writing – original draft; writing – review & editing.

Data availability

No primary research results, software or code have been included and no new data were generated or analysed as part of this review.

Conflicts of interest

There are no conflicts to declare.

Acknowledgements

This study was financed, in part, by the São Paulo Research Foundation (FAPESP), Brazil (Processes Numbers 22/14645-2 and 2016/02414-5 – MGO and 2022/13352-1 – MPB) and, in part, by the National Council for Scientific and Technological Development (CNPq) (Processes Numbers 141023/2022-8 – HVA and 142065/2021-8 – EHCS).

References

1 D. A. Riccio and M. H. Schoenfisch, *Chem. Soc. Rev.*, 2012, **41**, 3731–3741.
2 M. C. Jen, M. S. Serrano, R. van Lith and G. A. Ameer, *Adv. Funct. Mater.*, 2012, **22**, 239–260.
3 J. Kim, G. Saravanakumar, H. W. Choi, D. Park and W. J. Kim, *J. Mater. Chem. B*, 2014, **2**, 341.
4 Y. Yang, Z. Huang and L.-L. Li, *Nanoscale*, 2021, **13**, 444–459.
5 G. R. Navale, S. Singh and K. Ghosh, *Coord. Chem. Rev.*, 2023, **481**, 215052.
6 A. Haleem, M. Javaid, R. Hasan Khan and R. Suman, *J. Clin. Orthop. Trauma*, 2019, **11**, S118–S124.
7 G. Saini, N. Segaran, J. L. Mayer, A. Saini, H. Albadawi and R. Oklu, *J. Clin. Med.*, 2021, **10**, 4966.
8 Y. Bao, N. Paunović, J.-C. Leroux, Y. Bao, N. Paunović and J.-C. Leroux, *Adv. Funct. Mater.*, 2022, **32**, 2109864.
9 V. M. Vaz and L. Kumar, *AAPS PharmSciTech*, 2021, **22**, 1–20.
10 L. M. Estes Bright, Y. Wu, E. J. Brisbois and H. Handa, *Curr. Opin. Colloid Interface Sci.*, 2023, **66**, 101704.
11 M. Ganzarolli de Oliveira, *Basic Clin. Pharmacol. Toxicol.*, 2016, **119**, 49–56.
12 D. D. Thomas, L. A. Ridnour, J. S. Isenberg, W. Flores-Santana, C. H. Switzer, S. Donzelli, P. Hussain, C. Vecoli, N. Paolocci, S. Ambs, C. A. Colton, C. C. Harris, D. D. Roberts and D. A. Wink, *Free Radicals Biol. Med.*, 2008, **45**, 18–31.
13 T. P. Reddy, S. A. Glynn, T. R. Billiar, D. A. Wink and J. C. Chang, *Clin. Cancer Res.*, 2023, **29**, 1855–1868.
14 E. M. Hetrick and M. H. Schoenfisch, *Chem. Soc. Rev.*, 2006, **35**, 780–789.
15 N. Barraud, D. Schleheck, J. Klebensberger, J. S. Webb, D. J. Hassett, S. A. Rice and S. Kjelleberg, *J. Bacteriol.*, 2009, **191**, 7333–7342.
16 Y. Wu, M. R. Garren, L. M. Estes Bright, P. Maffe, M. Brooks, E. J. Brisbois and H. Handa, *J. Colloid Interface Sci.*, 2024, **653**, 1763–1774.
17 M. Champeau, V. Póvoa, L. Militão, F. M. Cabrini, G. F. Picheth, F. Meneau, C. P. Jara, E. P. de Araujo and M. G. de Oliveira, *Acta Biomater.*, 2018, **74**, 312–325.
18 F. Kabirian, P. Brouki Milan, A. Zamanian, R. Heying and M. Mozafari, *Acta Biomater.*, 2019, **92**, 82–91.
19 R. M. Clancy, P. F. Gomez and S. B. Abramson, *Osteoarthritis Cartilage*, 2004, **12**, 552–558.
20 T. A. Heinrich, R. S. Da Silva, K. M. Miranda, C. H. Switzer, D. A. Wink and J. M. Fukuto, *Br. J. Pharmacol.*, 2013, **169**, 1417–1429.
21 R. Vercelino, T. M. Cunha, E. S. Ferreira, F. Q. Cunha, S. H. Ferreira and M. G. De Oliveira, *J. Mater. Sci. Mater. Med.*, 2013, **24**, 2157–2169.
22 C. S. Martins, R. F. C. Leitão, D. V. S. Costa, I. M. Melo, G. S. Santos, V. Lima, V. Baldim, D. V. T. Wong, L. E. Bonfim, C. B. Melo, M. G. De Oliveira and G. A. C. Brito, *PLoS One*, 2016, **11**, e0153716.
23 J. Cao, M. Su, N. Hasan, J. Lee, D. Kwak, D. Y. Kim, K. Kim, E. H. Lee, J. H. Jung and J. W. Yoo, *Pharmaceutics*, 2020, **12**, 926.
24 S. Cuzzocrea, T. Persichini, L. Dugo, M. Colasanti and G. Musci, *Free Radicals Biol. Med.*, 2003, **34**, 1253–1262.
25 H. V. de Almeida, D. M. Catori, L. C. E. da Silva and M. G. de Oliveira, *Macromol. Symp.*, 2022, **406**, 2200047.

26 P. G. Wang, M. Xian, X. Tang, X. Wu, Z. Wen, T. Cai and A. J. Janczuk, *Chem. Rev.*, 2002, **102**, 1091–1134.
27 K. A. Broniowska and N. Hogg, *Antioxid. Redox Signal.*, 2012, **17**, 969–980.
28 C. Zhang, T. D. Biggs, N. O. Devarie-Baez, S. Shuang, C. Dong and M. Xian, *Chem. Commun.*, 2017, **53**, 11266–11277.
29 F. S. Schanuel, K. S. Raggio Santos, A. Monte-Alto-Costa and M. G. de Oliveira, *Colloids Surf., B*, 2015, **130**, 182–191.
30 B. Seabra, A. Fitzpatrick, J. Paul, M. G. De Oliveira and R. Weller, *Br. J. Dermatol.*, 2004, **151**, 977–983.
31 A. Joseph, C. W. McCarthy, A. G. Tyo, K. R. Hubbard, H. C. Fisher, J. A. Altscheffel, W. He, R. Pinnaratip, Y. Liu, B. P. Lee and R. M. Rajachar, *ACS Biomater. Sci. Eng.*, 2019, **5**, 959–969.
32 J. Dou, R. Yang, X. Jin, P. Li, X. Han, L. Wang, B. Chi, J. Shen and J. Yuan, *Regen. Biomater.*, 2022, **9**, rbac006.
33 M. Li, W. Qiu, Q. Wang, N. Li, L. Liu, X. Wang, J. Yu, X. Li, F. Li and D. Wu, *ACS Appl. Mater. Interfaces*, 2022, **14**, 15911–15926.
34 K. Park, J. I. Dawson, R. O. C. Oreffo, Y. H. Kim and J. Hong, *Biomacromolecules*, 2020, **21**, 2096–2103.
35 L. Tang, P. Wu, H. Zhuang, Z. Qin, P. Yu, K. Fu, P. Qiu, Y. Liu and Y. Zhou, *Int. J. Biol. Macromol.*, 2023, **241**, 124564.
36 S. Ghalei, M. Douglass and H. Handa, *ACS Biomater. Sci. Eng.*, 2022, **8**, 3066–3077.
37 H. Zhuang, J. Shao, P. Wu, G. Yu, K. Fu, Z. Sun, M. Cao, Y. Liu and Y. Zhou, *Int. J. Biol. Macromol.*, 2023, **224**, 1244–1251.
38 G. Zheng, R. Li, P. Wu, L. Zhang, Y. Qin, S. Wan, J. Pei, P. Yu, K. Fu, M. E. Meyerhoff, Y. Liu and Y. Zhou, *Int. J. Biol. Macromol.*, 2023, **252**, 126371.
39 N. Davari, J. Nourmohammadi and J. Mohammadi, *Int. J. Biol. Macromol.*, 2024, **265**, 131062.
40 S. M. Shishido, A. B. Seabra, W. Loh and M. G. De Oliveira, *Biomaterials*, 2003, **24**, 3543–3553.
41 H. Vieira de Almeida, L. C. Escobar da Silva and M. Ganzarolli de Oliveira, *Nitric Oxide*, 2024, **146**, 48–57.
42 S. Tripathi, S. S. Mandal, S. Bauri and P. Maiti, *MedComm*, 2023, **4**, e194.
43 Y. Yu, K. M. Fischenich, S. A. Schoonraad, S. Weatherford, A. C. Uzcategui, K. Eckstein, A. Muralidharan, V. Crespo-Cuevas, F. Rodriguez-Fontan, J. P. Killgore, G. Li, R. R. McLeod, N. H. Miller, V. L. Ferguson, S. J. Bryant and K. A. Payne, *npj Regen. Med.*, 2022, **7**, 1–14.
44 G. Zhou, H. Jiang, Z. Yin, Y. Liu, Q. Zhang, C. Zhang, B. Pan, J. Zhou, X. Zhou, H. Sun, D. Li, A. He, Z. Zhang, W. Zhang, W. Liu and Y. Cao, *EBioMedicine*, 2018, **28**, 287–302.
45 V. Mironov, N. Reis and B. Derby, *Tissue Eng.*, 2006, **12**, 631–634.
46 J. Groll, J. A. Burdick, D. W. Cho, B. Derby, M. Gelinsky, S. C. Heilshorn, T. Jüngst, J. Malda, V. A. Mironov, K. Nakayama, A. Ovsianikov, W. Sun, S. Takeuchi, J. J. Yoo and T. B. F. Woodfield, *Biofabrication*, 2018, **11**, 013001.
47 M. L. Bedell, A. M. Navara, Y. Du, S. Zhang and A. G. Mikos, *Chem. Rev.*, 2020, **120**, 10744–10792.
48 W. L. Ng, J. M. Lee, M. Zhou, Y. W. Chen, K. X. A. Lee, W. Y. Yeong and Y. F. Shen, *Biofabrication*, 2020, **12**, 022001.
49 S. Naghieh and X. Chen, *J. Pharm. Anal.*, 2021, **11**, 564–579.
50 R. Chaudhary, P. Fabbri, E. Leoni, F. Mazzanti, R. Akbari and C. Antonini, *Prog. Addit. Manuf.*, 2022, **8**, 331–351.
51 J. Huang, Q. Qin and J. Wang, *Processes*, 2020, **8**, 1138.
52 F. Puza, K. Lienkamp, F. Puza and K. Lienkamp, *Adv. Funct. Mater.*, 2022, **32**, 2205345.
53 H. Abu Owida, *Appl. Bionics Biomech.*, 2022, **2022**, 2260216.
54 D. M. Kirchmajer, R. Gorkin and M. In Het Panhuis, *J. Mater. Chem. B*, 2015, **3**, 4105–4117.
55 I. Seoane-Viaño, P. Januskaite, C. Alvarez-Lorenzo, A. W. Basit and A. Goyanes, *J. Controlled Release*, 2021, **332**, 367–389.
56 R. Pugliese, B. Beltrami, S. Regondi and C. Lunetta, *Ann. 3D Print. Med.*, 2021, **2**, 100011.
57 K. von Petersdorff-Campen, Y. Hauswirth, J. Carpenter, A. Hagmann, S. Boës, M. S. Daners, D. Penner and M. Meboldt, *Appl. Sci.*, 2018, **8**, 1275.
58 C. C. Chang, E. D. Boland, S. K. Williams and J. B. Hoying, *J. Biomed. Mater. Res., Part B*, 2011, **98**, 160–170.
59 S. Bom, R. Ribeiro, H. M. Ribeiro, C. Santos and J. Marto, *Int. J. Pharm.*, 2022, **615**, 121506.
60 A. Schwab, R. Levato, M. D'Este, S. Piluso, D. Eglin and J. Malda, *Chem. Rev.*, 2020, **120**, 11028–11055.
61 M. P. Bomediano, L. C. E. da Silva, P. Mota-Santiago, M. G. de Oliveira and T. S. Plivelic, *Front. Soft Matter*, 2024, **4**, 1354122.
62 W. Li, L. S. Mille, J. A. Robledo, T. Uribe, V. Huerta and Y. S. Zhang, *Adv. Healthc. Mater.*, 2020, **9**, 2000156.
63 G. Gillispie, P. Prim, J. Copus, J. Fisher, A. G. Mikos, J. J. Yoo, A. Atala and S. J. Lee, *Biofabrication*, 2020, **12**, 022003.
64 C. Yu, J. Schimelman, P. Wang, K. L. Miller, X. Ma, S. You, J. Guan, B. Sun, W. Zhu and S. Chen, *Chem. Rev.*, 2020, **120**, 10695–10743.
65 A. GhavamiNejad, N. Ashammakhi, X. Y. Wu and A. Khademhosseini, *Small*, 2020, **16**, 2002931.
66 Z. Gu, J. Fu, H. Lin and Y. He, *Asian J. Pharm. Sci.*, 2020, **15**, 529–557.
67 Z. Bashiri, M. Rajabi Fomeshi, H. Ghasemi Hamidabadi, D. Jafari, S. Alizadeh, M. Nazm Bojnordi, G. Orive, A. Dolatshahi-Pirouz, M. Zahiri, R. L. Reis, S. C. Kundu and M. Gholipourmalekabadi, *Mater. Today Bio*, 2023, **20**, 100666.
68 Z. Bashiri, M. Rajabi Fomeshi, H. Ghasemi Hamidabadi, D. Jafari, S. Alizadeh, M. Nazm Bojnordi, G. Orive, A. Dolatshahi-Pirouz, M. Zahiri, R. L. Reis, S. C. Kundu and M. Gholipourmalekabadi, *Mater. Today Bio*, 2023, **20**, 100666.
69 K. Trabbic-Carlson, L. A. Setton and A. Chilkoti, *Biomacromolecules*, 2003, **4**, 572–580.

70 S. Tripathi, S. S. Mandal, S. Bauri and P. Maiti, *MedComm*, 2023, **4**, e194.
71 J. R. H. Joseph Rey, Q. Chen, R. D. Maalihan, J. Ren, Í. G. M. da Silva, N. P. Dugos, E. B. Caldona and R. C. Advincula, *MRS Commun.*, 2021, **11**, 197–212.
72 Y. Ding, L. Warlick, M. Chen, E. Taddese, C. Collins, R. Fu, C. Duan, X. Wang, H. Ware, C. Sun and G. Ameer, *Bioact. Mater.*, 2024, **38**, 195–206.
73 T. R. Yeazel-Klein, A. G. Davis and M. L. Becker, *Adv. Mater. Technol.*, 2023, **8**, 2201904.
74 I. Chiesa, C. De Maria, M. R. Ceccarini, L. Mussolin, R. Coletta, A. Morabito, R. Tonin, M. Calamai, A. Morrone, T. Beccari and L. Valentini, *ACS Appl. Mater. Interfaces*, 2022, **14**, 19253–19264.
75 D. M. Catori, M. V. Lorevice, L. C. E. da Silva, G. Candido, A. L. G. Millás and M. G. de Oliveira, *Macromol. Symp.*, 2022, **406**, 2200050.
76 C. M. Pavlos, H. Xu and J. P. Toscano, *Curr. Top. Med. Chem.*, 2005, **5**, 637–647.
77 S. D. M. Lourenço and M. G. de Oliveira, *J. Photochem. Photobiol., A*, 2017, **346**, 548–558.
78 M. J. Malone-Povolny, S. E. Maloney and M. H. Schoenfisch, *Adv. Healthc. Mater.*, 2019, **8**, 1801210.
79 Y. Wu, T. Liang, Y. Hu, S. Jiang, Y. Luo, C. Liu, G. Wang, J. Zhang, T. Xu and L. Zhu, *Regen. Biomater.*, 2021, **8**, 1–10.
80 V. C. O. Póvoa, G. J. V. P. dos Santos, G. F. Picheth, C. P. Jara, L. C. E. da Silva, E. P. de Araújo and M. G. de Oliveira, *Tissue Eng. Regener. Med.*, 2020, **14**, 807–818.
81 J. E. Freedman and J. Loscalzo, *J. Thromb. Haemostasis*, 2003, **1**, 1183–1188.
82 F. Kabirian, B. Ditkowski, A. Zamanian, M. F. Hoylaerts, M. Mozafari and R. Heying, *ACS Biomater. Sci. Eng.*, 2019, **5**, 2284–2296.
83 F. Kabirian, P. Baatsen, M. Smet, A. Shavandi, P. Mela and R. Heying, *Sci. Rep.*, 2023, **13**, 1–12.
84 M. K. Chug, E. Bachtiar, N. Narwold, K. Gall and E. J. Brisbois, *Biomater. Sci.*, 2021, **9**, 3100–3111.
85 J. E. Won, W. J. Kim, J. S. Shim and J. J. Ryu, *Macromol. Biosci.*, 2022, **22**, 2200162.
86 R. J. Van't Hof and S. H. Ralston, *Immunology*, 2001, **103**, 255–261.
87 Q. Yang, H. Yin, T. Xu, D. Zhu, J. Yin, Y. Chen, X. Yu, J. Gao, C. Zhang, Y. Chen and Y. Gao, *Small*, 2020, **16**, 1906814.
88 M. F. de Oliveira, L. C. E. da Silva and M. G. de Oliveira, *Bioprinting*, 2021, **22**, e00137.
89 M. F. de Oliveira, L. C. E. da Silva, D. M. Catori, M. V. Lorevice, K. E. A. Galvão, A. L. G. Millás and M. G. de Oliveira, *Macromol. Biosci.*, 2023, **23**, 2200448.
90 M. I. Santos, L. C. E. da Silva, M. P. Bomediano, D. M. Catori, M. C. Gonçalves and M. G. de Oliveira, *Soft Matter*, 2021, **17**, 6352–6361.
91 F. Rong, Y. Tang, T. Wang, T. Feng, J. Song, P. Li and W. Huang, *Antioxidants*, 2019, **8**, 556.
92 W. Li, Y. Yang, C. J. Ehrhardt, N. Lewinski, D. Gascoyne, G. Lucas, H. Zhao and X. Wang, *ACS Appl. Bio Mater.*, 2021, **4**, 7653–7662.
93 P. D. Wood, B. Mutus and R. W. Redmond, *Photochem. Photobiol.*, 1996, **64**, 518–524.
94 D. M. Catori, L. C. E. da Silva, M. F. de Oliveira, G. H. Nguyen, J. C. Moses, E. J. Brisbois, H. Handa and M. G. de Oliveira, *ACS Appl. Mater. Interfaces*, 2023, **15**, 48930–48944.
95 H. Goodarzi Hosseinabadi, D. Nieto, A. Yousefinejad, H. Fattel, L. Ionov and A. K. Miri, *Appl. Mater. Today*, 2023, **30**, 101721.
96 A. Blaeser, D. Filipa Duarte Campos, U. Puster, W. Richtering, M. M. Stevens, H. Fischer, A. Blaeser, D. F. Duarte Campos, U. Puster, H. Fischer, W. Richtering and M. M. Stevens, *Adv. Healthc. Mater.*, 2016, **5**, 326–333.
97 M. A. Kuss, S. Wu, Y. Wang, J. B. Untrauer, W. Li, J. Y. Lim and B. Duan, *J. Biomed. Mater. Res., Part B*, 2018, **106**, 1788–1798.
98 A. Joshi, S. Choudhury, S. B. Gugulothu, S. S. Visweswariah and K. Chatterjee, *Biomacromolecules*, 2022, **23**, 2730–2751.

